Constraining the ship contribution to the aerosol of the Central Mediterranean

S. Becagli[1], F. Anello[2], C. Bommarito[2], F. Cassola[3,4], G. Calzolai[5], T. Di Iorio[6], A. di Sarra[6], J.L. Gómez-Amo[6,7], F. Lucarelli[5], M. Marconi[1], D. Meloni[6], F. Monteleone[2], S. Nava[5], G. Pace[6], M. Severi[1], D. M. Sferlazzo[8], R. Traversi[1], and R. Udisti[1]

[1] Department of Chemistry, University of Florence, Sesto Fiorentino, Florence, I-50019, Italy
[2]ENEA, Laboratory for Earth Observations and Analyses, Palermo, I-90141, Italy
[3]Department of Physics & INFN, University of Genoa, Genoa, I-16146, Italy.
[4]ARPAL-Unità Operativa CFMI-PC, Genova, I-16129, Italy.
[5]Department of Physics, University of Florence & INFN-Firenze, Sesto Fiorentino, Florence, I-50019, Italy.
[6]ENEA Laboratory for Earth Observations and Analyses, Roma, I-00123, Italy
[7]Department of Earth Physics and Thermodynamics, University of Valencia, Spain.
[8]ENEA, Laboratory for Earth Observation and Analyses, Lampedusa, I-92010, Italy

Keywords: ship aerosol, Central Mediterranean Sea, PM_{10}, La-Ce ratio, Vanadium.

Abstract

PM_{10} aerosol samples were collected during summer 2013 within the framework of the Chemistry and Aerosol Mediterranean Experiment (ChArMEx) at two sites located North (Capo Granitola) and South (Lampedusa Island), respectively, of the main Mediterranean shipping route in the Sicily Channel.
The PM_{10} samples were collected with 12 hour time resolution at both sites. Selected metals, main anions, cations, and elemental and organic carbon were determined.
The evolution of soluble V and Ni concentrations (typical markers of heavy fuel oil combustion) was related to meteorology and ship traffic intensity in the Sicily Channel, using a high resolution regional model for calculation of back trajectories. Elevated concentration of V and Ni at Capo Granitola and Lampedusa are found to correspond with airmasses from the Sicily Channel and coincidences between trajectories and positions of large ships; the vertical structure of the planetary boundary layer also appears to play a role, with high V values associated with strong inversions and stable boundary layer. The V concentration was generally lower at Lampedusa than at Capo Granitola, where it reached a peak value of 40 ng/m^3.
Concentrations of rare earth elements, La and Ce in particular, were used to identify possible contributions from refineries, whose emissions are also characterized by elevated V and Ni amounts; refinery emissions are expected to display high La/Ce and La/V ratios, due to the use of La in the fluid catalytic converter systems. In general, low La/Ce and La/V ratios were observed in the PM samples. The combination of the

analyses based on chemical markers, arimass trajectories, and ship routes allows to unambiguously identify the large role of the ship source in the Sicily Channel.
Based on the sampled aerosols, ratios of the main aerosol species arising from ship emission with respect to V were estimated with the aim of deriving a lower limit for the total ship contribution to PM_{10}. The estimated minimum ship emission contributions to PM_{10} was 2.0 $\mu g/m^3$ at Lampedusa, and 3.0 $\mu g/m^3$ at Capo Granitola, corresponding to 11% and 8.6% of PM_{10}, respectively.

1. Introduction

Ship emissions may significantly affect atmospheric concentrations of several important pollutants, especially in maritime and coastal areas (e.g. Endresen et al., 2003). Main emitted compounds are carbon dioxide (CO_2), nitrogen oxides (NO_x), sulfur dioxide (SO_2), carbon monoxide (CO), hydrocarbons, and primary and secondary particles. Thus, ship emissions impact the greenhouse gas budget (Stern, 2007), acid rain (through NO_x and SO_2 oxidation products; Derwent at al., 2005), human health (CO, hydrocarbons, particles; Lloyd's Register Engineering Services, 1995; Corbett et al., 2007) and solar radiation budget through aerosol direct and indirect effects (black carbon and sulfur containing particles; Devasthale et al., 2006; Lauer et al., 2007; Coakley and Walsh, 2002).
Heavy oil fuels used by ships contain varying transition metals. The aerosol emitted by ship engines is formed at high temperature (>800°C) from V, Ni, Fe compounds (Sippula et al., 2009). The thermodynamics predicts that the metals in these particles are mainly present as oxides. Sulfuric acid is found to form a liquid layer on the metal oxide ultrafine particles, leading to the metal partial dissolution, probably increasing the toxicity of the particles when inhaled.
In spite of the large amount of gas and particulate emitted by ships, maritime transport is relatively clean if calculated per kilogram of transported good. However, maritime transport has been increasing with respect to air and road transport (Micco and Pérez, 2001; Grewal and Haugstetter, 2007). In addition, emissions from other transport sectors are decreasing due to the implementation of advanced emission reduction technologies, and the relative impact of shipping emissions is increasing.
Regulations aiming at reducing emissions based on restrictions on the fuel sulfur content (sulfur emission control areas, SECAs) have been implemented in several regions. Although the legislation is focussed on sulfur emissions, the overall health and environmental effects depend in complex way on the physical and chemical properties of the emissions (WHO, 2013). Several studies have been carried out to determine the detailed chemical composition of shipping emissions (Agrawal et al., 2008a and b, Moldanová et al., 2009, Murphy et al., 2009, Lyyränen et al 1999, Cooper, 2003, Sippula et al. 2014); however, , the ships emissions are still poorly characterized with respect to on-road vehicles.

A large variety of anthropic sources (refineries, power plants, intense ship traffic, etc.) and natural emissions make the Mediterranean region one of the most polluted in the world (e.g., Kouvarakis et al., 2000; Marmer and Langmann, 2005). The multiplicity of Mediterranean sources (some of which with the same markers of ship aerosol) makes difficult the quantification of ship contribution to the total aerosol amount (e.g., Becagli et al., 2012).

The contribution of ships and harbour emissions to local air quality, with specific focus on atmospheric aerosol, has been investigated using models (Trozzi et al., 1995; Gariazzo et al., 2007; Eyring et al., 2005; Marmer et al., 2009), experimental analyses at high temporal resolution (Ault et al., 2010; Contini et al., 2011; Jonsson et al., 2011; Diesch et al., 2013; Donateo et al., 2014), receptor models based on the identification of chemical tracers associated with ship emissions (Viana et al., 2009; Pandolfi et al., 2011; Cesari et al., 2014), and integrated approaches with receptor and chemical transport models (Bove et al., 2014). Few studies exist in open sea (Becagli et al., 2012; Schembari et al., 2014; Bove et al., 2016).

In this context, studies performed at Mediterranean sites, where it is possible to distinguish ship emission from other sources of heavy fuel oil combustion, are important to investigate the current impact of the ship emissions on primary and secondary aerosols. This study contributes to the identification and characterization of the emissions from ships and the impact on the aerosol distribution in the central Mediterranean. The experiment was set up with the aim of unambiguously recognizing the ship source by a combination of methods.

2. Measurements and methods

In a previous study (Becagli et al., 2012) we used measurements of PM_{10} concentration and chemical composition carried out at Lampedusa to investigate the role of ship emissions in the central Mediterranean. Vanadium and Nickel were used as tracers of heavy fuel combustion together with trajectory analyses to assess the role of ship traffic. The ship source, however, could not be unequivocally separated from possible influences from refineries and power plants, which use similar fuels. In summer 2013 we addressed the same topic by implementing a specific strategy to target the aerosols due to ship emissions. PM_{10} samples were collected in parallel at Lampedusa (LMP) and at Capo Granitola (CGR), i.e., respectively South and North of the main shipping route through the Mediterranean, with the aim of isolating the ship source. The chemical analyses of the collected samples were complemented with measurements of Rare Earth Elements (REEs), trajectories and planetary boundary layer information from a high resolution regional model, and actual observations of ship traffic. The combination of these approaches allows to unambiguously identify the ship source, and permits to constrain its contribution to PM_{10} in the central Mediterranean.

The PM_{10} samples were collected in summer 2013 as a contribution to the Chemistry and Aerosol Mediterranean Experiment (ChArMEx; http://charmex.lsce.ispl.fr). Lampedusa is one of the supersites of the ChArMEx experiment; a list of the

instruments deployed during the special observing period 1a of ChArMEx, and of the measurement strategy, meteorological conditions, and main observations is given by Mallet et al. (2016).

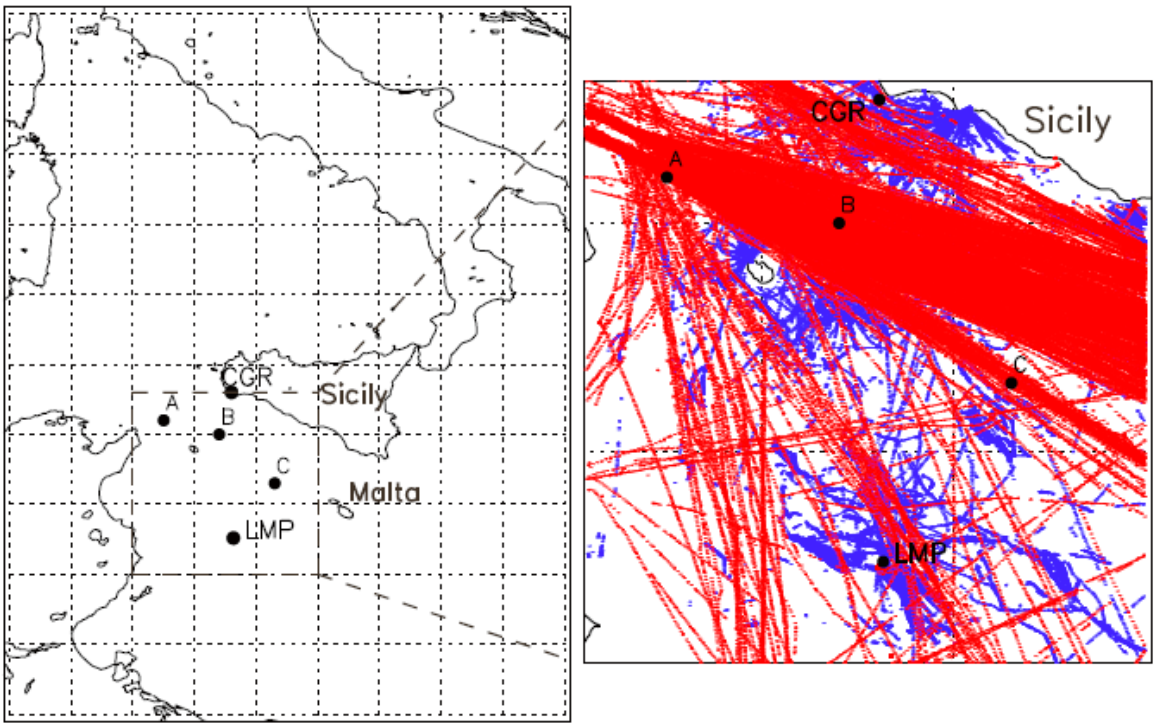

Figure 1. Map of the study area with the sites of Lampedusa (LMP) and Capo Granitola (CGR) (left panel). A, B, and C indicate the three sites selected to study the stability of the boundary layer in the Sicily Channel (see section 3.2.2). The ship routes in the study area during the first 10 days of June 2013 are displayed in the right panel. Red and blue dots show the routes of merchant and fishing vessels, respectively.

2.1. Aerosol sampling and chemical analyses

PM_{10} was sampled at two sites: at the Station for Climate Observations, maintained by ENEA (the Italian Agency for New Technologies, Energy, and Sustainable Economic Development) on the island of Lampedusa (35.5°N, 12.6°E), and at the Italian CNR (National Research Council) Research Centre at Capo Granitola (36.6°N, 12.6° E).
Lampedusa is a small island in the Central Mediterranean sea, more than 100 km far from the nearest Tunisian coast. At the Station for Climate Observations, which is located on a 45 m a.s.l. plateau on the North-Eastern coast of Lampedusa, continuous observations of aerosol properties (di Sarra et al., 2011, 2015; Becagli et al., 2013; Marconi et al., 2014; Calzolai et al., 2015; Sellitto et al., 2017), aerosol radiative effects (e.g., Casasanta et al., 2011; di Sarra et al., 2011; Meloni et al., 2015), and other

climatic parameters are carried out. Figure 1 shows the map of the central Mediterranean with the measurement stations.

PM_{10} is routinely sampled on a daily basis at LMP (Becagli et al., 2013; Marconi et al., 2014; Calzolai et al., 2015) by using a low volume dual channel sequential sampler (HYDRA FAI Instruments) equipped with two PM_{10} sampling heads operating in accord with UNI EN12341. For the intensive ChArMEx campaign, samples were collected at 12-hour resolution (8:00-20:00 and 20:00-8:00 local time) from 1 June to 3 August, 2013.

The two channels operated in parallel and were loaded with different types of filters: the first one with 47 mm diameter, 2 µm nominal porosity Teflon filters, and the second one with 47 mm pre-fired, 2 µm nominal porosity, quartz filters. Ion chromatographic analysis of soluble ions, atomic emission spectroscopy for soluble metals, and proton-induced X-ray emission (PIXE) for the total (soluble+insoluble) elemental composition were carried out on the Teflon filters. Elemental (EC) and organic carbon (OC) were measured by analysing the quartz filters.

The sampling site at CGR is located at Torretta Granitola, a Research Center of the Italian National Research Council, in South-Western Sicily (12 km from Mazara del Vallo). The sampler was installed on the roof of one of the research centre buildings at about 20 m a.s.l., directly on the coastline, facing the strait of Sicily.

At CGR PM_{10} samples were collected at 12 hour resolution (8:00-20:00 and 20:00-8:00 local time) with a TECORA Skypost sequential sampler on 47 mm pre-fired 2 µm nominal porosity quartz filters, which were used to determine ions, metals, EC and OC on different fractions of the filter. Due to technical problems, some daytime (8:00-20:00) samplings were lost at CGR.

The PM_{10} mass was determined by weighting the filters before and after sampling with an analytical balance in controlled conditions of temperature (20±1 °C) and relative humidity (50±5 %). The estimated error on PM_{10} mass is around 1% at 30 $\mu g/m^3$ in the applied sampling conditions.

A quarter of each Teflon filter from LMP and a 1.5 cm^2 punch of the quartz filter from CGR were analysed by Ion Chromatography (IC) in the analytical conditions described in Marconi et al. (2014). The estimated uncertainty for IC measurements is 5% for all the considered ions.

Blank values were negligible with respect to the concentration in the samples for Teflon filters. Blank values for quartz filters were negligible for most of the analyzed species. For some species characterized by high blank values, always lower than the 25^{th} percentile value, they were subtracted from the measured concentrations.

Another quarter of the Teflon filter from LMP, and another 1.5 cm^2 punch of the quartz filter from CGR were extracted in ultrasonic bath for 15 min with MilliQ water acidified at pH 1.5–2 with ultrapure HNO_3 obtained by sub-boiling distillation. This extract was used for the metals soluble part determination by means of an Inductively Coupled Plasma Atomic Emission Spectrometer (ICP-AES, Varian 720-ES) equipped with an ultrasonic nebulizer (U5000 AT+, Cetac Technologies Inc.). The pH chosen value is the lowest found in rainwater (Li and Aneja, 1992) and leads to the determination of the

metals fraction available to biological organisms and, for some metals (e.g. V and Ni), related to the anthropic source (Becagli et al., 2012).

The remaining half Teflon filter from Lampedusa another punch of the quartz filter from CGR were used for the determination of metals by ICP-AES through the solubilisation procedure reported in the EU EN14902 (2005) rule, by using concentrated sub-boiling distilled HNO_3 and 30% ultrapure H_2O_2 in a microwave oven at 220°C for 25 min (P = 55 bar). This solubilisation procedure is not able to completely dissolve the silicate species. However, this procedure allows to recover at least 70% of the same elements measured by proton induced X ray emission technique also for elements with dominant crustal source (unpublished data), due to the low crustal aerosol load in these sampling period (e.g., Mailler et al., 2016). La and Ce presented very low concentrations in the collected aerosol samples. Thus, particular attention was devoted to the minimization of the La and Ce detection limit. In the used sampling and analytical conditions of LMP samples the detection limits for La and Ce are 0.02 ng/m^3 and 0.08 ng/m^3, respectively, and are about 4 times higher for the CGR samples, due to the smaller filter portion used for the analysis.

The OC and EC measurements were carried out on a 1.5 cm^2 punch of the quartz filters from Lampedusa and Capo Granitola by means of a Sunset thermo-optical transmittance analyser, following the NIOSH protocol (Wu et al, 2016).

The overall aerosol sampling and analytical strategy for the two sites are reported in table 1.

Table 1. Sampling strategy and chemical measurements carried out on each filter for the two sites: Lampedusa (LMP) and Capo Granitola (CGR).

Sampling site	**Filter**	**Sampling interval, local time.**	**Measurements**
LMP	Teflon	8:00-20:00 (daytime sample)	• PM_{10}; • Ions by IC (1/4 of the filter); • metals in HNO_3 pH 1.5 room temperature extract by ICP-AES (1/4 of the filter); • metals in HNO_3-H_2O_2 in microwave oven extract by ICP-AES (1/2 filter)
		20:00-8:00 (nighttime sample)	
	Quartz	8:00-20:00 (daytime sample)	• EC/OC by thermo-optical analyser (1.5 cm x 1 cm punch)
		20:00-8:00 (nighttime	

		sample)	
CGR	Quartz	8:00-20:00 (daytime sample)	• PM_{10}; • Ions by IC (1.5 cm x 1 cm punch); • metals in HNO_3 pH 1.5 room temperature extract by ICP-AES (1.5 cm x 1 cm punch); • metals in HNO_3-H_2O_2 in microwave oven extract by ICP-AES (1.5 cm x 1 cm punch) • EC/OC by thermo-optical analyser (1.5 cm x 1 cm punch)
		20:00-8:00 (nighttime sample)	

2.3. Atmospheric model and trajectory calculations

Numerical simulations with a non-hydrostatic mesoscale atmospheric model were used to characterize the meteorological conditions in the Sicily Channel during the campaign and to support the interpretation of the experimental results. The Weather Research and Forecasting (WRF) model (Skamarock et al., 2008) outputs, provided by the Department of Physics of the University of Genoa, Italy, were used, covering the entire Mediterranean with a grid spacing of 10 km and hourly temporal resolution. Initial and boundary conditions to drive WRF simulations were obtained from the Global Forecast System operational global model (Environmental Modeling Center, 2003) outputs (0.5x0.5 squared degrees). Some recent applications of the modelling chain are described in Mentaschi et al. (2015) and Cassola et al. (2016), where full details on the model configuration can also be found.

In particular, the WRF 3-D hourly meteorological fields were used to calculate backward trajectories with the NOAA HYbrid Single-Particle Lagrangian Integrated Trajectory Model (HYSPLIT; Stein et al. 2015). The trajectories were used to assess the origin of the air masses impacting the monitoring sites and to support the source attribution suggested by the analysis of specific markers (see Section 3.2.2). The use of a high-resolution regional atmospheric model for trajectory calculations allows a better representation of boundary layer properties and mesoscale phenomena such as land/sea breezes, which can have a relevant impact especially in complex topography coastal sites like CGR.

Also, the high temporal resolution of meteorological data (hourly instead of three- or six-hourly products typically available from global models) permits a better description of diurnal cycles as well as a more accurate trajectory computation, without time interpolation between subsequent atmospheric fields (Solomos et al., 2015).

Specifically, 48-h long back trajectories arriving at LMP and CGR were computed from a reference height of 10 m above the ground level, starting every six hours for the whole period of the campaign, from 10 June to 31 July, 2013.

2.4. Ships/marine traffic

Position and main characteristics of the ships travelling in the central Mediterranean were derived from the MarineTraffic database (http://www.marinetraffic.com/), which provides data with a high temporal resolution (about 3-5 minutes) by means of the Automatic Identification System (AIS).
Three classes of ships defined by the AIS classification were considered: all the ships, the merchant (i.e. cargo and tanker), and the fishing vessels. Merchant and fishing vessels are the most frequent ships in the Sicily Channel; merchant ships are expected to produce the highest impact due to their higher emissions (http://ec.europa.eu/environment/archives/air/pdf/chapter2_ship_emissions.pdf).

3. Results

3.1. PM_{10} chemical composition at the two sites

The sea salt aerosol (SSA) component of PM_{10} was estimated as the sum of Na^+, Mg^{2+}, Ca^{2+}, K^+, sulfate and chloride sea salt (ss) fractions. Details on the calculation of sea salt Na^+ and Ca^{2+}, and non-sea salt (nss) fractions are reported in Marconi et al. (2014). The Mg^{2+}, Ca^{2+}, K^+, and sulphate sea salt fractions were calculated from sea salt Na^+ ($ssNa^+$) by using the ratio of each component to Na^+ in bulk sea water: $Mg^{2+}/Na^+ = 0.129$, $Ca^{2+}/Na^+ = 0.038$, $K^+/Na^+ = 0.036$, $SO_4^{2-}/Na^+ = 0.253$ (Bowen, 1979). Chloride undergoes depletion processes during aging of sea spray, mainly due to exchange reactions with anthropogenic H_2SO_4 and HNO_3, leading to re-emission of gaseous HCl in the atmosphere. Thus, for chloride we use the measured chloride concentration instead of the one calculated from $ssNa^+$. Thus,

$$SSA = 1.46 * [ssNa^+] + [Cl^-].$$

The crustal component is calculated from Al, which represents 8.2% of the upper continental crust, UCC (Henderson and Henderson 2009). A previous study using an extensive data set at Lampedusa showed that the crustal content determined from the total Al was in very good agreement with calculations made from the sum of the metal oxides (Marconi et al., 2014). However, in this study we use measurements of the soluble Al concentration obtained by ICP-AES on the solution obtained with H_2O_2 and HNO_3 in microwave oven instead of the total Al content. Therefore, in this work we underestimate the crustal contribution by about 30% (unpublished results). However, it must be emphasized that the crustal aerosol contribution was very low throughout the measurement campaign.

Figure 2 shows the time series of the main PM_{10} components at LMP and CGR. An intense Mistral event occurred from 22 June to 1 July. Mistral events are characterized

by strong winds from the north-westerly sector, and often by subsiding air masses originating from the free troposphere (Jiang et al., 2003). Thus, elevated values of SSA and low concentrations of other compounds are generally found during Mistral at Lampedusa.

Average concentrations of PM_{10} and of the different aerosol components for the whole measurement campaign and for the non-Mistral conditions are reported in Table 2. The averages were calculated over a homogeneous dataset, i.e., when measurements are available at both sites.

Table 2. Mean and standard deviation of PM_{10} load and composition, and percentage with respect to PM_{10} (in bracket) at Lampedusa and Capo Granitola. Mean, standard deviation and percentage are calculated on homogeneous data sets for both sites considering all the common sampling ("all data" columns) and excluding the mistral events ("Mistral excluded" columns).

	Lampedusa		**Capo Granitola**	
	All data	**Mistral excluded**	**All data**	**Mistral excluded**
PM_{10} ($\mu g/m^3$)	18.0±6.6	16.3±5.2	34.1±18.9	27.2±6.5
Sea Salt Aerosol ($\mu g/m^3$)	4.63±6.30 (25.7%)	2.33±3.21 (14.3%)	8.14±15.50 (23.9%)	2.12±6.51 (7.8%)
Crustal Aerosol ($\mu g/m^3$)	0.82±0.44 (4.6%)	0.90±0.43 (5.5%)	2.80±1.7 (8.2%)	3.02±1.75 (11.1%)
$nssSO_4^{2-}$ ($\mu g/m^3$)	3.95±2.28 (21.9%)	4.40±2.22 (27.0%)	6.78±3.08 (19.9%)	7.53±2.78 (27.7%)
NH_4^+ ($\mu g/m^3$)	0.98±0.56 (5.5%)	1.09±0.55 (6.7%)	1.48±0.94 (4.3%)	1.66±0.87 (6.1%)
NO_3^- ($\mu g/m^3$)	1.25±1.00 (7.0%)	1.02±0.02 (6.2%)	1.35±1.11 (4.0%)	1.01±0.82 (3.7%)
Organic aerosol ($\mu g/m^3$)	3.86±1.56 (21.4%)	4.04±1.59 (24.8%)	9.02±2.52 (26.5%)	9.53±2.29 (35.0%)
Elemental carbon ($\mu g/m^3$)	0.15±0.08 (0.8%)	0.15±0.08 (0.9%)	0.44±0.28 (1.3%)	0.51±0.26 (1.9%)
Unknown ($\mu g/m^3$)	2.52±3.26 (14.0%)	2.20±3.40 (13.5%)	4.11±7.78 (12.1%)	1.82±4.48 (6.7%)

The largest PM_{10} values were associated with elevated SSA during the Mistral event at both sites. PM_{10} is about two times larger at Capo Granitola than at Lampedusa. The PM_{10} measured during the campaign at Lampedusa was significantly lower than its long-term average (31.5 $\mu g/m^3$; Marconi et al., 2014). No Saharan dust transport events occurred at low altitude in this period (e.g., Mailler et al., 2015), and the crustal aerosol contribution remained very low and almost constant at both sites (average < 1 $\mu g/m^3$ at LMP and around 3 $\mu g/m^3$ at CGR corresponding to 4.6% and 8.2% of the PM_{10} at LMP and CGR respectively).

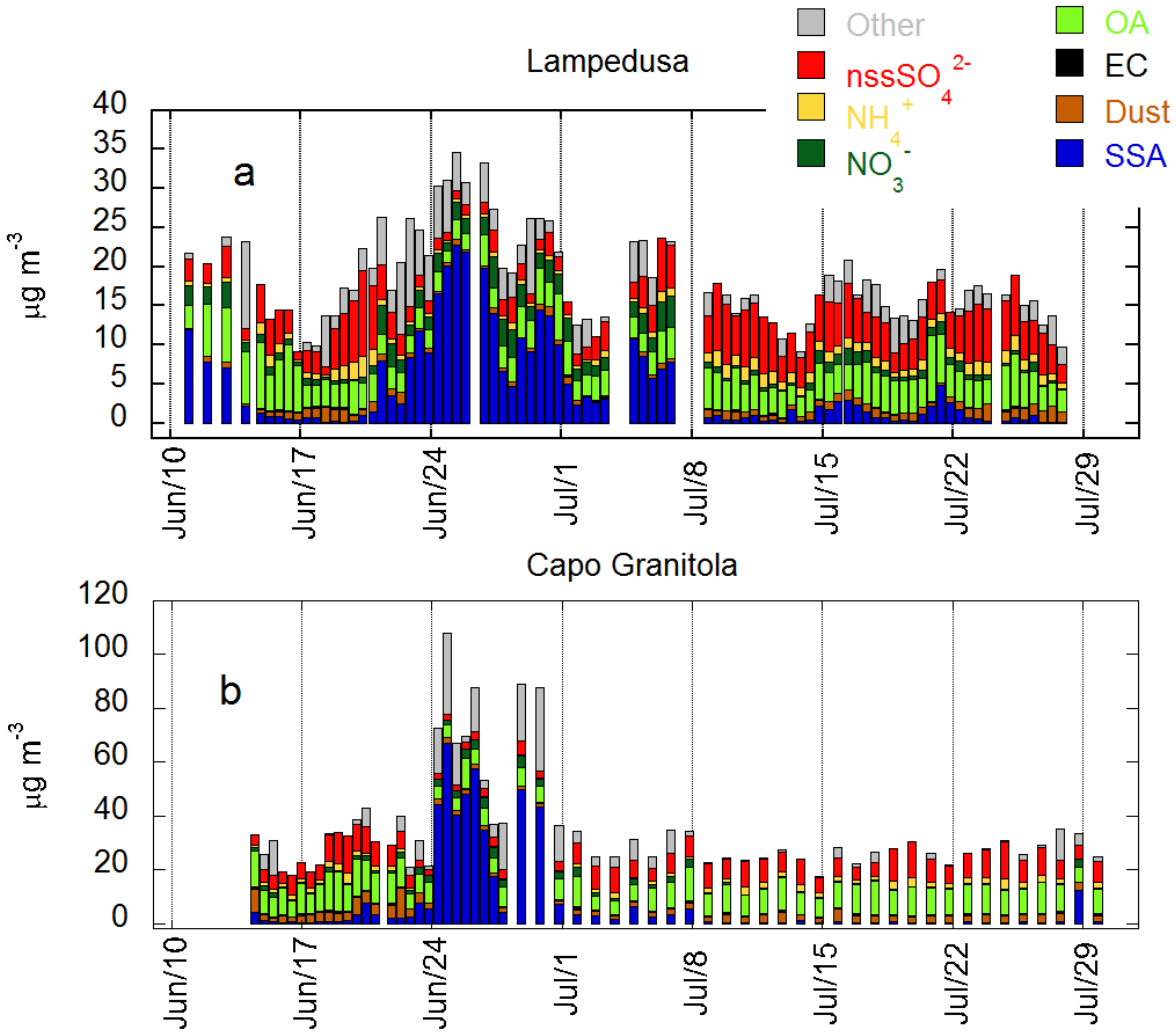

Figure 2. Time series of the main aerosol components at LMP (plot a) and CGR (plot b). Note the different vertical scales of the graphs. OA stands for organic aerosol.

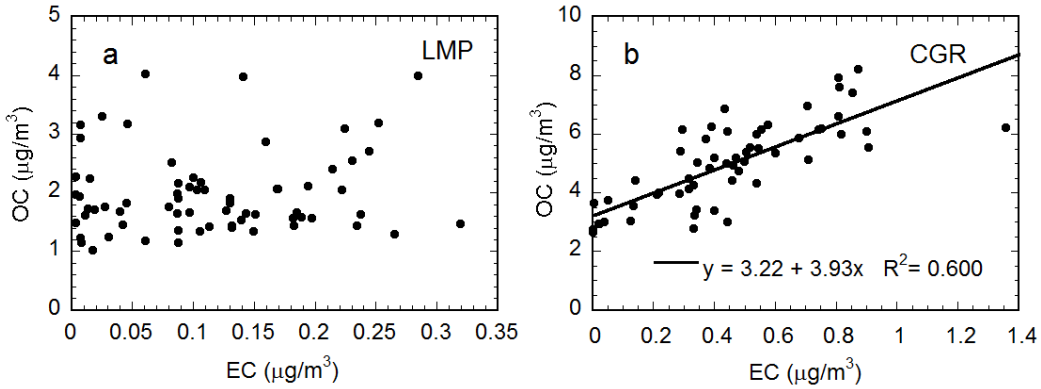

Figure 3. Scatter plot of OC vs. EC at LMP (plot a) and CGR (plot b). Note the different vertical scales.

SSA accounted for about 26% and 24% of PM_{10} at LMP and CGR, respectively. The SSA contribution was about 14% of PM_{10} at LMP and 8% at CGR during the periods not influenced by the Mistral. Non-sea salt SO_4^{2-} was the most abundant among the secondary inorganic species.

Nitrate concentrations, although relatively high at both sites, are in agreement with the long term measurements performed at Lampedusa (e.g., Calzolai et al., 2015) and with data from other remote sites in the western (Mallorca; e.g. Simo et al., 1991) and eastern Mediterranean (Finokalia; e.g. Mihalopoulos et al., 1997).

Organic aerosol (OA) was the most abundant component at CGR, where its mean concentration was > 9 $\mu g/m^3$ and represented 35% of PM_{10} in the days not characterized by Mistral.

Elemental carbon and organic carbon show higher values at CGR than LMP. At CGR moderate and elevated values of OC and EC appear correlated (R^2=0.60; n =59; Figure 3b), suggesting a strong influence from carbon species primary sources, characterized by the simultaneous EC and OC emission. The influence from primary sources is apparent at EC > 0.4 $\mu g/m^3$. At LMP, on the contrary, OC was not correlated with EC (figure 3a), indicating a strong impact of OC secondary and/or natural sources. This confirms that Lampedusa may be considered a background site in the central Mediterranean (see e.g., Artuso et al., 2009; Henne et al., 2010), and the observations there may be taken as representative for a relatively wide open sea region.

Thus, we used a conversion factor of 1.8 (typical for urban background sites, Turpin and Lin, 2001) at CGR, and of 2.1 (typical for remote sites characterized by high impact of secondary sources, Turpin and Lin, 2001) at LMP to estimate the total organic aerosol amount from the OC measured values. Once estimated OA with this method, the sum of the various species accounted to more than 85% of the measured mass at

both sites. The unreconstructed mass could be due to an underestimation of OA from OC, or to the presence of bound water not removed by the desiccation procedure at 50% relative humidity (Tsyro, 2005; Canepari et al., 2013).

3.1.1. Ship emission markers: V and Ni

Several studies focussed on the identification of shipping emissions specific tracers (Viana et al., 2008; Becagli et al., 2012, Isakson et al., 2001, Hellebust et al., 2010). Vanadium and Nickel are generally considered the best markers for this source because, after sulfur, they are the main impurities in heavy fuel oil (Agrawal et al., 2008a and b). The soluble fraction of these metals is even more representative for the ship source (Becagli et al., 2012).

Following Becagli et al. (2012), we used measurements of the V and Ni soluble fractions (V_{sol} and Ni_{sol}, respectively). In the data set here considered the V_{sol} and Ni_{sol} ratio with respect to Al were always more than 10 times larger than for UCC, as expected for cases dominated by heavy oil combustions sources (ships, refineries, power plants, stainless steel production plants).

Table 3 reports slope, correlation coefficient, and number of samples of the linear correlation between V_{sol} and Ni_{sol}.

Table 3. Correlation parameters between V and Ni at LMP and CGR PM_{10} samples for all the samples and for samples with V concentration higher than 6 ng/m^3.

		Slope (± uncertainty)	R^2	n.
LMP	All data	2.94±0.03	0.986	124
	V_{sol} > 6ng/m^3	2.99±0.03	0.994	44
CGR	All data	2.82±0.08	0.950	59
	V_{sol} > 6ng/m^3	3.00±0.05	0.989	34

V_{sol} and Ni_{sol} are highly correlated, suggesting a common source. The obtained slope of the regression line (2.8-2.9, that increases to 3.0 for samples with V_{sol} >6 ng/m^3) is in the range of ratios typical for heavy fuel oil combustion sources. The same value was found at Lampedusa by Becagli et al. (2012), considering data from 2004 to 2008. The behaviour of V, Ni, and their ratio are then representative of heavy fuel oil combustion. It must be emphasized that the V/Ni ratio is expected to display a large variability due to varying fuel composition and engine operating conditions (Mazzei et al., 2008; Agrawal et al., 2008a and b, Viana et al. 2009; Pandolfi et al., 2011). It is however difficult to distinguish V and Ni originating from power plants, refineries, or ship

engines. Moreover, several refineries are present in Sicily (Siracusa, Gela, Milazzo) and in Sardinia (Cagliari) and may potentially influence the sampling sites.
A combination of methods is thus used in this study to unequivocally identify the ship source. The analysis is based on: additional chemical tracers, like the Rare Earth Elements, whose behaviour is specific for the refinery and the ship sources; high resolution back-trajectories, based on data from the high resolution regional model; information on the vertical mixing in the atmospheric boundary layer; coincidences between the high resolution back-trajectories and the position of different types of ships in the Sicily Channel.

3.1.2. Rare Earth elements

As discussed above, anthropogenic V and Ni originate from heavy oil combustion, and may be considered markers of the ship source only when other sources can be excluded. Few studies propose the use of lanthanoid elements (La to Lu) to distinguish refinery from ship emissions (Moreno et al., 2008a and b; Du and Turner, 2015; Kulkarni et al., 2006).
In particular, the ratio between the La and Ce concentrations (La/Ce ratio, hereafter LCR) and between La and V (hereafter LVR) can be used to identify specific sources. Shipping emissions are characterised by values of LCR between 0.6 and 0.8 and LVR < 0.1 (Moreno et al., 2008a, 2008b).
Crustal aerosols are characterized by LCR ranging from 0.4 to 0.6 and LVR usually in the range 0.2-0.3 (Moreno et al., 2008 a and b). LCR depends weakly on differences in dust source area and collected aerosol size fraction, contrarily to LVR, which reaches 0.9 for large (>10 μm) particles from specific areas of Sahara (e.g., Hoggar Massif; Handerson and Handerson, 2009; Moreno et al., 2006; Castillo et al, 2008).
Elevated values of LCR (from 1 to 13) are associated with emissions from refineries (Moreno et al., 2008a; Du and Turner, 2015). This is because zeolitic fluidised-bed catalytic cracking (FCC) unit enriched in La are used to crack long-chain olefins in crude oil to shorter-chain products (Bozlaker et al., 2016; Du and Turner 2015; Kulkani et al 2006; Moreno et al., 2008a, 2008b).
Mixing of aerosol from different sources may produce a large variability of LCR, with larger values corresponding to a stronger impact from refineries.
The time series of LCR and LVR at LMP and CGR are displayed in figure 4. The range of values expected for crustal aerosol is highlighted in the figure. Please, note that the uncertainty on LCR is very large when La and Ce concentrations are close to the measurement detection limit. These cases may produce very large values of LCR which are not significant; these cases were removed from the time series.
LCR at LMP and CGR was generally around the value expected for crustal aerosol (dashed grey area in figure 4); 10 samples from LMP and 2 samples from CGR show values LCR higher than 1. LCR is >1.5 in a single case, at LMP. .This suggests that the refineries impact is small in the collected samples.

Moreno et al. (2008b) have shown that it is possible to identify aerosol from refineries based on V, La, Ce three-component plot. This type of plot is shown in figure 5 for the data from LMP and CGR. La and Ce were scaled in order to have the typical UCC composition in the centre of the plot.

The compositions of UCC (Henderson and Henderson, 2009), African desert dust (Castillo et al., 2008; Moreno et al., 2006), FCC (Kulkarni et al., 2006), La-contaminated (refinery) Asian dust collected at Mauna Loa, Hawai'i (Olmez and Gordon, 1985), and PM_{10} and $PM_{2.5}$ collected at Puertollano (Spain) in days possibly affected by refinery emissions (Moreno et al., 2008b) are also displayed in figure 5.

The data from CGR and LMP are grouped in a region with elevated values of V, and La and Ce generally lower than for refinery and dust cases.

Data from Puertollano shown in figure 5 are relative to days characterized by winds originating from sectors where refineries are located; however, these samples are affected by a mix of particles from several sources, including refineries. Aerosol samples from Spain affected in most cases display larger La to Ce and La to V ratios than those found at LMP and CGR. The composition of all samples collected in this period at LMP is consistent with a large impact from ship emissions. Some cases at CGR may suggest the simultaneous occurrence of crustal and ship aerosols, or dominant crustal component (orange open dots in figure 5). Therefore, these cases display a relatively low V concentration and are mainly associated with the Mistral event. A limited crustal contamination may possibly occur at CGR in these cases, due to resuspension due to the strong wind.

Cases with LCR>1 (grey and pink open circle for CGR and LMP respectively) are highlighted in figure 5. The aerosol composition is however consistent with the ship source also in these cases, suggesting that the impact of refineries is limited.

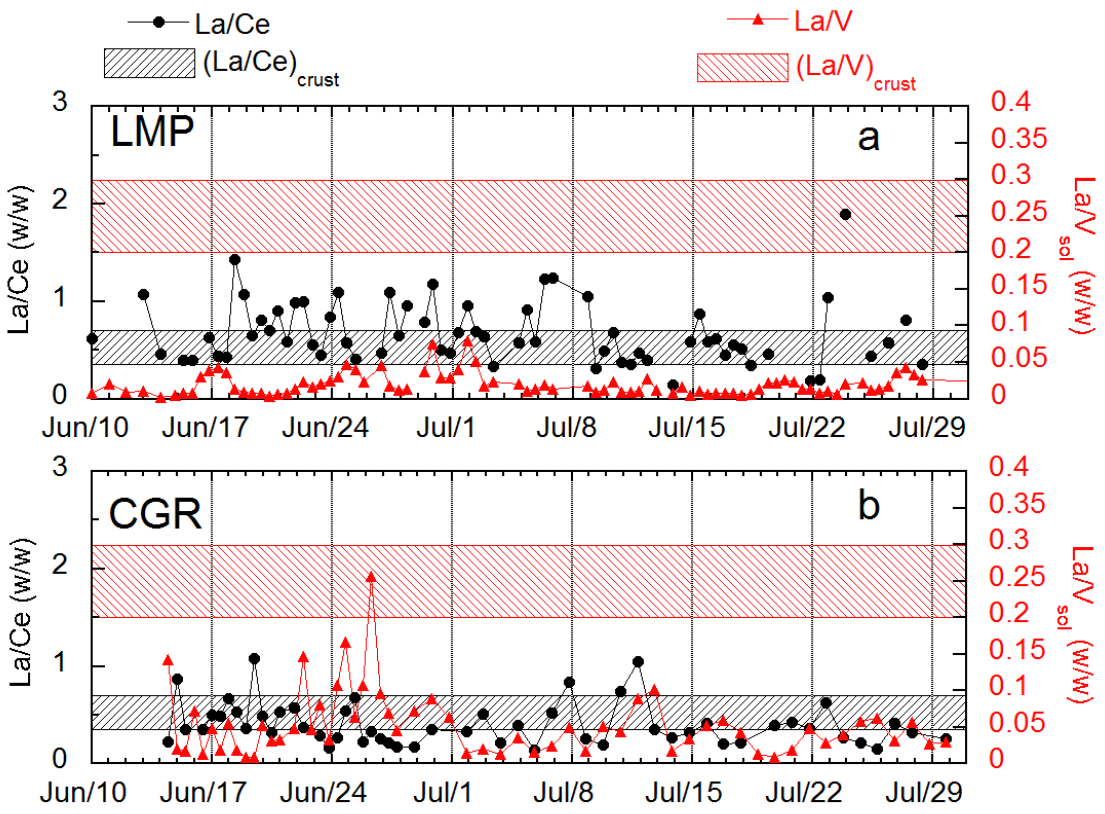

460
461
462 Figure 4. Time series of LCR and LVR at a), Lampedusa, and b), Capo Granitola. The
463 horizontal red and grey shadow areas in each plot represent the ranges of values for
464 upper continental crust LVR and LCR, respectively.
465

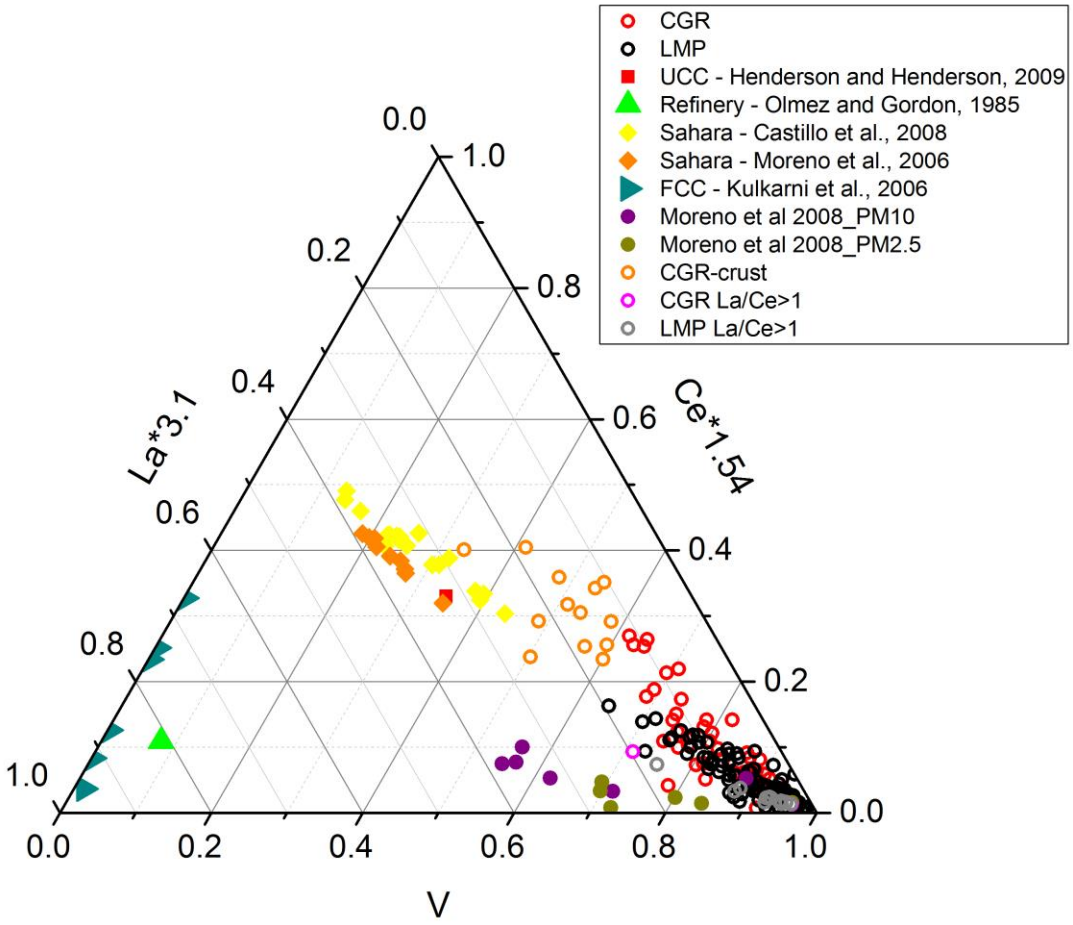

Figure 5. Three-component Ce-La-V plots for LMP and CGR. Literature data for different aerosol types are also shown.

3.2. Trajectories and ship traffic

3.2.1 Origin of air masses during the campaign

All the trajectories arriving at LMP and CGR, calculated with the HYSPLIT model driven by WRF meteorological fields (see Section 2.3), are shown in an aggregated way in Figure 6, where the trajectory frequency at each point of the computing grid is shown for the whole period (upper panels) and for the 10 – 30 June interval (lower panels). The trajectory frequency pattern is elongated in the NW-SE direction at LMP, while it is distributed over a wider range of directions at CGR, despite a general prevalence of northerly sectors. The predominance of air masses coming from the northwest is particularly evident in June (lower panels); when areas with trajectory frequencies exceeding 10% are found farther to the north, up to the Gulf of Lion.

During the first part of the campaign (June 2013) the synoptic situation was characterized by a "dipolar" sea level pressure anomaly pattern, with positive anomalies in the western Mediterranean and negative ones in the eastern part of the basin (Denjean et al., 2016). This situation induced stronger and more frequent than usual north-westerly winds (i.e. Mistral episodes, see Section 3.1) over the Sardinia and Sicily Channels.

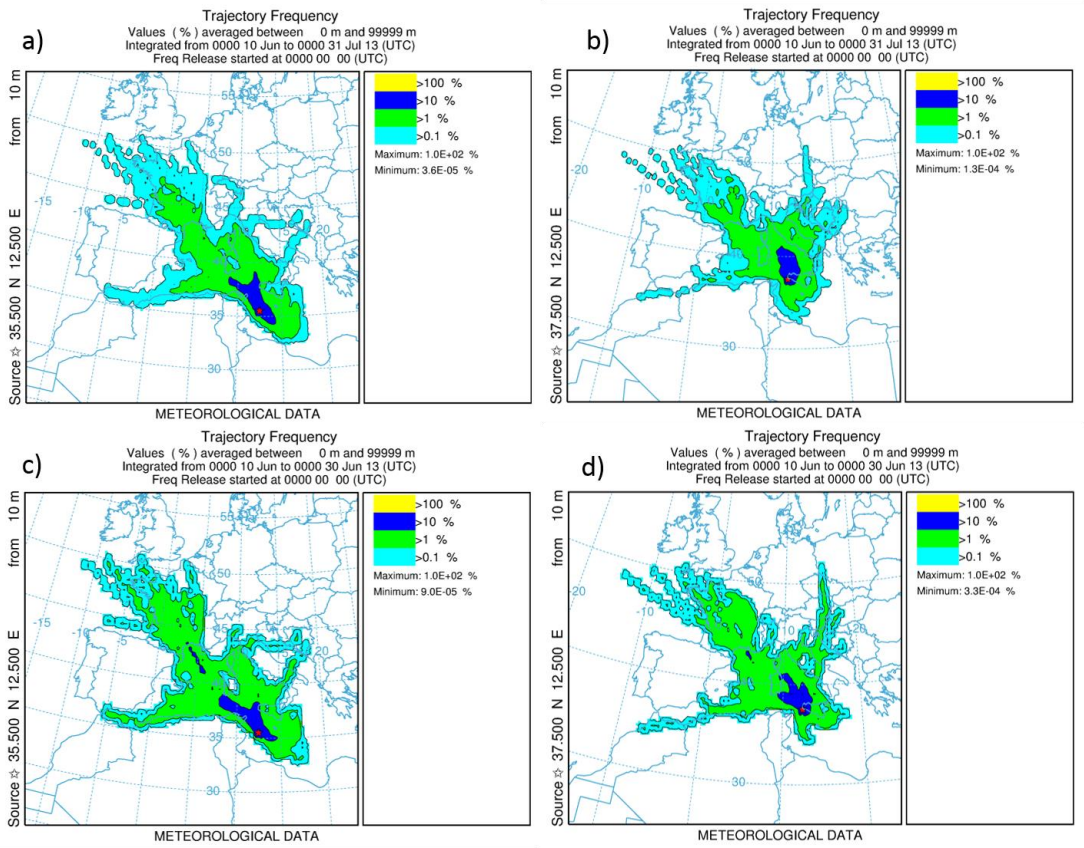

Figure 6. Trajectory frequency computed at each grid cell with starting points at LMP (panels a, c) and CGR (b, d). Upper panels show values averaged over the whole period of the campaign (10 June – 31 July 2013), while lower panels are relative to the 10-30 June interval.

3.2.2 Ship traffic

To further investigate the mechanisms determining the presence of ship emissions markers at the two sites we investigated the relationships among the amount of V, the back-trajectory pattern, the effective number of ships influencing the air mass, the stability of the boundary layer in the ship source region (i.e., the Sicily Channel), and the REE to V ratios discussed in section 3.1.2.

All back-trajectories arriving at LMP and CGR were considered and all trajectory-ship coincidences occurring within the last 36 hours before sampling were taken into account.

It was assumed that the ship plume influenced the sampled air mass if:

- the trajectory passed within 15 km of the position of a ship
- the corresponding air mass altitude was less than 500 m.

The total number of ships fulfilling these criteria was associated with each trajectory. The analysis was based on the available 1-hour time resolution meteorological fields (a ship influencing a trajectory was counted once every hour).

To further explore the impact of different types of ships, the analysis was carried out considering the following three ship categories: all the ships, the merchant (i.e. cargo and tanker), and the fishing vessels.

The atmospheric stability is also expected to play a large role in modulating the ship impact (see e.g., its influence on V amounts, Becagli et al. 2012). A temperature inversion, TI, index, was calculated based on the 3D atmospheric fields of the WRF model at three sites in the Sicily Channel. The temperature inversions were used as a proxy to identify periods characterized by a stable boundary layer. The three sites, A (37.2°N, 11.5°E), B (37.0°N, 12.4°E), and C (36.3°N, 13.3°E) (figure 1) were selected in the regions of most frequent ship passage and crossing with the trajectories from LMP and CGR. The TI index was calculated as the difference between the temperature at the altitude of the maximum T, and at the surface. A positive TI indicates an inversion, and the TI value provides an indication of the inversion strength. Only positive values are considered in this analysis.

Figure 7 summarizes the results of this analysis. It shows the time series of the number of the ships influencing the trajectories arriving at LMP and CGR, respectively, and the corresponding measured values of V. Samples which show a limited influence from ship emissions, determined on the basis of the La-Ce-V composition (see section 3.1.2), are highlighted with arrows (orange arrows for samples with La-Ce-V ratios typical for crust; pink and gray for sample possibly influenced by refineries, i.e., with LCR>1). Results are shown for the three classes of ships. The positive values of TI are also shown.

In general, there is a rather good correspondence between the cases classified as influenced by ships emissions and the number of ships encountered along the associated air mass trajectory at CGR. The correspondence is somewhat less evident at LMP. As discussed above, the V concentration ascribed to ships (data points without arrows n figure 7) is generally higher at CGR than at LMP. Part of this difference may be ascribed to the shorter distance between CGR and the main shipping route crossing the Sicily Channel with respect to Lampedusa, the consequent larger number of encountered ships, and an aerosol dilution effect during transport from the sources to LMP.

Maxima of V attributed to ships occurred between 19 and 20 June at CGR (about 42 ng/m^3), and on 21 June at LMP (36.1 ng/m^3). Similar concentrations were measured at CGR also around 18-19 July, in conjunction with an increase in the number of merchant

vessels. The 18-21 June period is the only event with high V concentrations quasi simultaneously at both sites. This is due to the peculiar circulation patterns, with airmass trajectories from the marine sector South of Sicily to CGR, and from the Sicily channel to LMP, particularly on 18 and 19 June. The 19-21 June episode is the largest occurring at LMP, both for duration and V concentration. Especially at the beginning of the event, large values of V do not correspond with an increase of the number of ships along the air mass trajectories.

A possible explanation for this behaviour is provided by the temporal evolution of TI in the Sicily Channel. The temperature inversion started to develop on 14 June, and gradually increased in intensity until 22 June; the TI persistence and progressive increase in intensity provided suitable conditions for the ship plumes trapping in the boundary layer, with a consequent build-up of the ship aerosol and V concentration. This process appears particularly efficient at CGR between 21 and 25 June.

A similar combined dependency on number of ships and TI appears also at LMP around 7 July. It is interesting to note that V from ships seems to depend more directly on the number of merchant ships (see, e.g., the lack of V peaks on 17 June, 12 and 29 July at LMP, when the number of fishing vessels was high and the number of merchant ships was low) than on the total or the fishing ships.

Thus, the trajectory analysis carried out in combination with the available information on the ship tracks confirms that the ship emissions are the main responsible for most of the moderate and elevated values of V measured at LMP and CGR during the campaign, and in particular for those cases with La and Ce compatible with the ship source. This analysis also clearly suggests that the boundary layer structure plays a very important role in determining the impact produced by the emissions. This simplified approach confirms the importance to carefully characterize the emission scenario and the meteorological conditions in studies on the ships emissions impact on air quality.

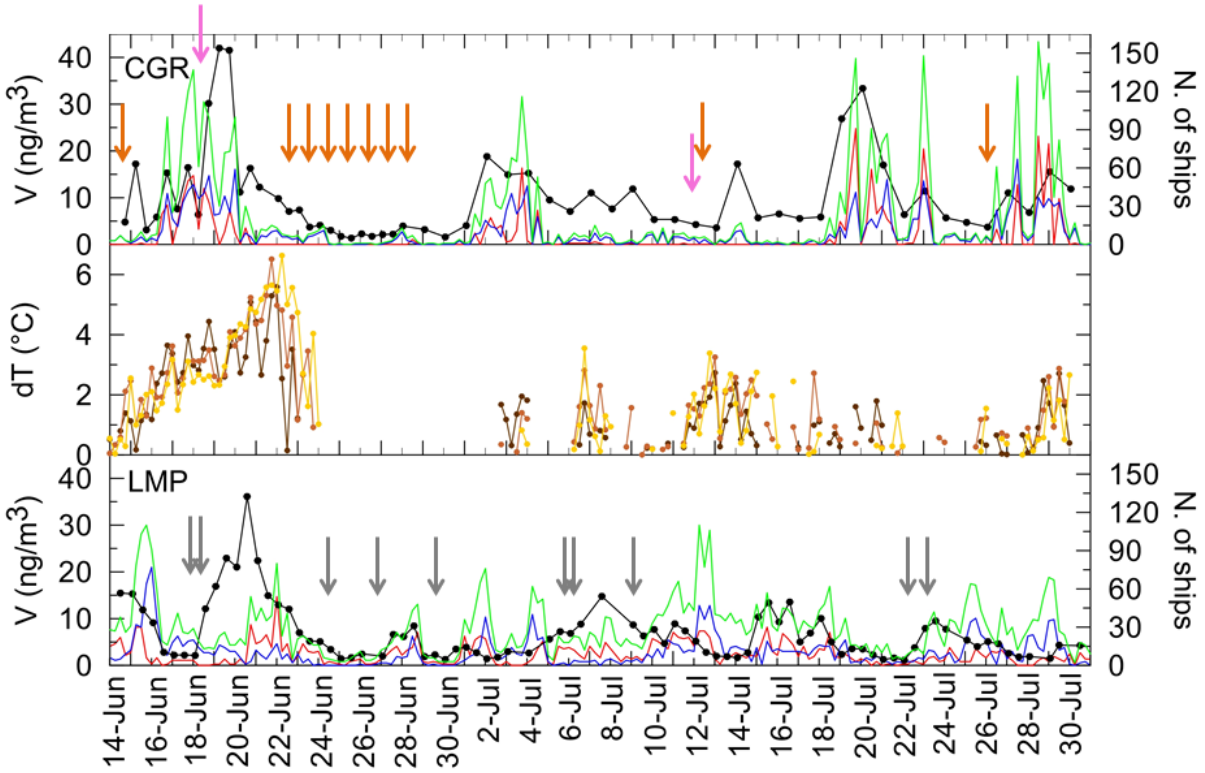

Figure 7. Time series of Vanadium concentration (black line with dots) and number of ships affecting the air masses sampled at CGR (upper panel) and LMP (lower panel). Green, red, and blue lines indicate respectively the total number of ships, the number of merchant (i.e. cargo and tanker), and of fishing vessels. The time evolution of the temperature inversion index (dT in the figure) at three different locations in the Sicily Channels is shown in the middle panel; brown, red, and yellow curves show the behaviour at sites A, B, and C (see text). The orange arrows identify samples classified as crustal based on the La-Ce-V concentration; pink and gray identify samples with LCR>1, possibly influenced by refineries.

3.3. Sulfate, nitrate, and organic carbon from ships

SO_2 is one of the main species emitted in the ship plume in the gas phase (Agrawal et al., 2008a, b). SO_2 is produced through oxidation of the S contained as impurity in heavy fuel oil, and is an aerosol precursor.

A previous study based on 5 years of data from Lampedusa (Becagli et al., 2012) has shown that the non-sea salt sulfate behaviour is not directly correlated with V and Ni

because several other SO_4^{2-} sources (anthropogenic, marine biogenic, crustal, volcanic) contribute to the non-sea salt sulfate in the Central Mediterranean Sea.

The same study suggested a lower limit of about 200 for the $nssSO_4^{2-}/V$ ratio for particles originating from heavy oil combustion at Lampedusa.

Figure 8 shows $nssSO_4^{2-}/V$ versus V at LMP and CGR. At both sites $nssSO_4^{2-}/V$ decreases for increasing V and reaches a lower limit at elevated values of V (> 15 ng/m^3). The analysis on REE, trajectories and ship traffic has shown that all samples with V > 15 ng/m^3 are strongly influenced by ships, and we assume that the ship emission is the dominant source of the sampled particles for these cases. This implies that in these cases virtually all sulfate originated from the ship source, and the observed lower limit for $nssSO_4^{2-}/V$ can be considered the lower limit for the sulfate to V ratio in the ship plume. Thus, to derive a lower limit for this ratio we calculate the mean and standard deviation of $nssSO_4^{2-}/V$ for V > 15 ng/m^3. The mean ratio and the mean ratio minus one standard deviation are shown in figure 8.

The $nssSO_4^{2-}$ to V ratio may still be decreasing for V around 15 ng/m^3, and we used a limit value equal to the average minus one standard deviation (dashed red lines in figure 8) to estimate the minimum expected contribution from ships to the total sulfate amount.

The calculated lower limit of the sulfate to V ratio at LMP is 207, in agreement with the values of 200 estimated by Becagli et al. (2012). The $nssSO_4^{2-}/V$ limit value at CGR, 323, is larger than at LMP. This difference is may be due to the contribution of other sulfate sources which may contribute to the $nssSO_4^{2-}$ even at high V concentration, and to the smaller distance from the ship source with respect to LMP. This result highlights the importance of remote sites like LMP to obtain information on the open Mediterranean.

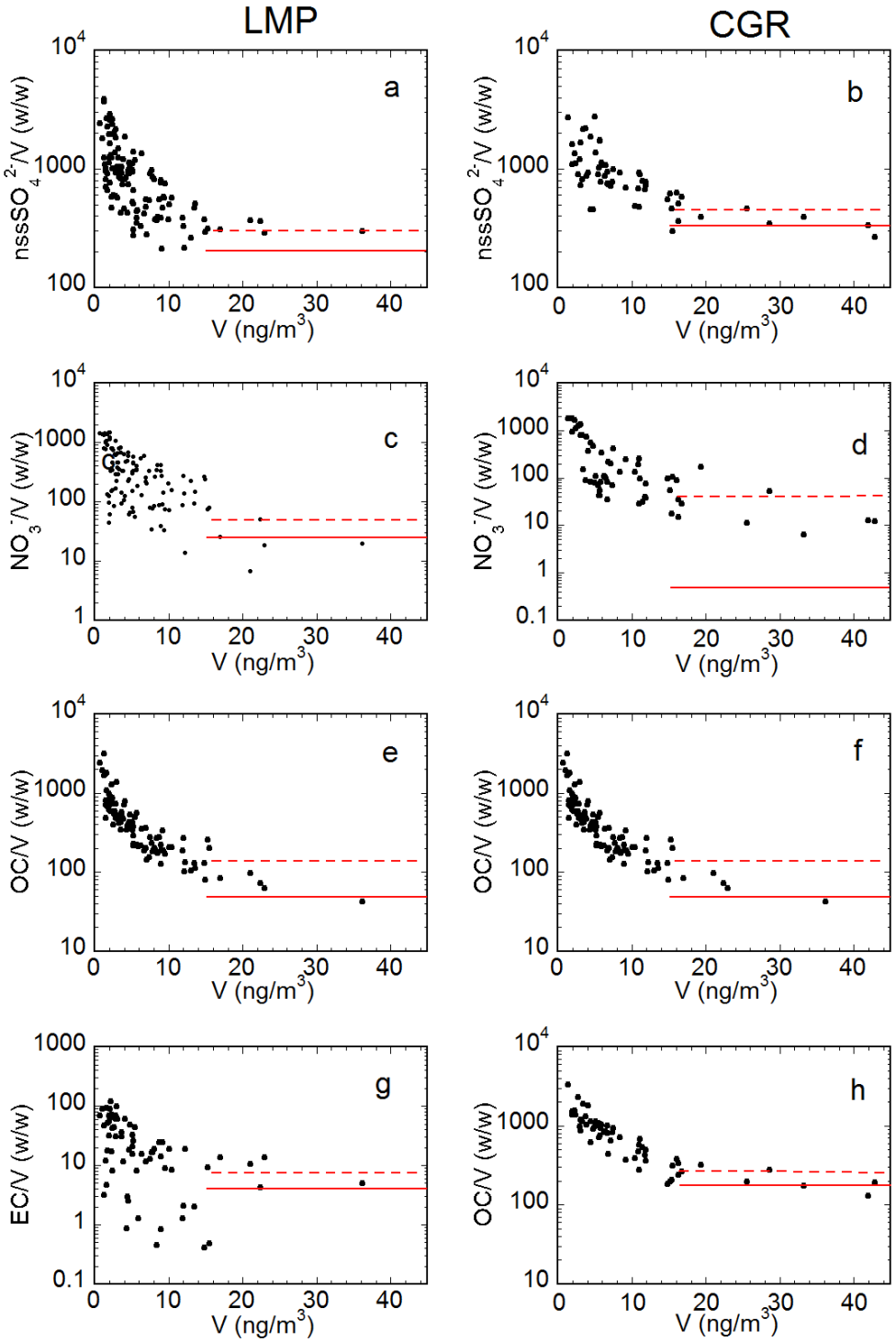

Figure 8. Scatter plots of $nssSO_4^{2-}/V$ (a and b), NO_3^-/V (c and d), OC/V (e and f) and EC/V (g and h) vs. V concentration at LMP (plots on the left) and CGR (plots on the right). The red lines in the plots represent the average (dashed line) and the average minus one standard deviation (solid line) calculated for samples with V>15 ng/m^3.

NOx are among the main compounds emitted in the gas phase acting as aerosol precursors. The photochemistry of NO_x leading to NO_3^- formation in the particulate phase is complex, especially in summer due to the presence of high amounts of OH radical (see e.g., Chen et al., 2005), and the NOx contribution to the particulate phase is not easy to be quantified.

Here we try to use the same approach used for sulfate for the determination of a lower limit for the NO_3^-/V ratio in the ship plume.

Figure 8 (plot c and d) shows the NO_3^-/V ratio versus V at the two sites. Similarly to sulfate, the average value of NO_3^-/V for V > 15 ng/m^3 is larger at CGR than at LMP. However, the standard deviation at CGR is significantly larger at CGR. The NOx concentration in the ship plume close to the source is larger than that of SO_2 and is strongly dependent on the engine operating conditions (Agrawal et al 2008b). The NOx lifetime is extremely low (1.8 hours during daytime and 6.5 hour during nighttime, Chen et al., 2005). However, the NO_3^-/V limit ratio values is low compared to the limit ratio for SO_4^{2-}. It has to be considered that NO_3^- takes part in other photochemical atmospheric reactions that lead to its removal. In addition, the presence of HNO_3 in gas phase not neutralized by NH_3 or by sea salt could explain the low $NO_3^-/nssSO_4^{2-}$ ratio in the aerosol. Indeed, the NO_3^- concentration measured at LMP and CGR is 4-6 times lower than that of $nssSO_4^{2-}$ (table 1). Low amounts of NO_3^- with respect to SO_4^{2-} from ship emissions are found in model simulations in Southern California (Dabdub, 2008). Indeed, Dabdub (2008) shows that the aerosol contribution from ship emissions is 0.05% for NO_3^-, and 44% for SO_4^{2-}.

Elemental and Organic Carbon are also present in the ship plume (Shah et al., 2004). In particular, OC constitutes about 15-25% and EC is generally lower than 1% of the PM sampled at the plume of main ship engine powered by heavy fuel oil (Agrawal et al., 2008b).

Figure 8 shows EC/V and OC/V versus V at LMP and CGR. Similarly to sulfate and nitrate, OC/V decreases with increasing V and reaches a minimum value for V > 15 ng/m^3 (43.1 and 179 at LMP and CGR, respectively) As discussed in section 3.1, other OC sources in addition to ships are present at CGR even at high values of V.

The pattern of the ratio EC/V versus V is less clear; in particular, several very low values of EC/V appear also at small values of V. This result is unexpected because V and EC are both markers of the primary ship aerosol, but the data here presented seem to suggest that non negligible EC contributions from other sources were present at CGR and that different fractionating effects acted during the transport. Also in this case the limit value is lower at LMP than at CGR.

Finally, as the limit ratios at CGR are likely affected by other sources than ship, we assume that the limit ratios obtained at Lampedusa for V>15 ng/m^3 are more representative of cases dominated by ship emissions during summer in a wide region. For this reason, the retrieved lower limits at LMP are used to quantify the ship contribution also at CGR.

3.4 Contribution of the ship aerosol to PM_{10}

With all the limitations above described, by using the lower limits for the ratios ($nssSO_4^{2-}$/V), (NO_3^-/V), and (OC/V) representative for ship aerosol it is possible to estimate the minimum contribution of $nssSO_4^{2-}$, NO_3^- and OC emitted by ships to the total budget of these components, and also to the total PM_{10} mass. It has to be noticed that the aerosol quantification obtained by this method is a rough estimate useful to constrain the ship aerosol contribution. In addition, due to possibly different meteorological conditions and photochemical activity, these values may vary spatially and seasonally.

The minimum ratio of each specie with respect to V, the minimum estimated contribution of ship emissions, for the average amount and for the maxima, to the total concentration of these species and to PM_{10}, are reported in Table 4. As previously discussed, the measured OC contribution is multiplied by 2.1 at LMP and by 1.8 at CGR to obtain the total organic aerosol contribution.

The estimated minimum concentration of non-sea-salt sulfate from ship emissions was 1.35 μg/m^3 on average during this campaign at LMP. This value is lower than in the previous study by Becagli et al. (2012) obtained over a longer period (2004-2008). The relative contribution to the total sulfate is however similar here and in Becagli et al. (2012), suggesting a similar role of $nssSO_4^{2-}$ from ship emissions to the total $nssSO_4^{2-}$ budget. The study by Becagli et al. (2012) covered an extended time period (2004-2008); the consistency with that study suggests that the results obtained during ChArMEx are not specific of summer 2013, but are representative for a wider temporal and spatial range.

At CGR the minimum ship contribution to sulfate, averaged over the same time period, is higher than at LMP (2.1 μg/m^3), but this higher value corresponds to a lower contribution to the total $nssSO_4^{2-}$, confirming that other $nssSO_4^{2-}$ sources are important at CGR.

Marmer and Langmann (2005) estimate that ship emissions contribute by 50% to the total amount of $nssSO_4^{2-}$ in the Mediterranean. This value is, as expected, larger than the estimated minimum contribution we derive (about 30%).

The estimated minimum contribution by ships to the total $nssSO_4^{2-}$ for cases with the largest ship impact (i.e. highest V concentration) is 69% and 77% at LMP and CGR, respectively.

Ships appear to contribute by small fractions to the total budget of NO_3^-. As previously mentioned, the NO_3^- atmospheric chemistry is complex and the contribution of nitrate from ship emission could be highly variable, especially in the Mediterranean region where high amount of UV radiation and highly reactive radical species are present.

Organic aerosol from ships also contributes significantly to the total OA amount and to the total PM; in particular, at LMP virtually all the OA present in cases with maximum ship impact may be attributed to the ship source.

By summing these three contributions, it is possible to estimate the total aerosol mass due to ship emissions, and its contribution to the total mass of PM_{10}. The lower limit for

the ship contribution was 2.0 μg/m^3 and 3.0 μg/m^3, corresponding to 11% and 8.6% of PM_{10} at LMP and CGR, respectively.

Table 4. Estimates of the average and maximum of the lower limit of $nssSO_4^{2-}$, NO_3^-, OA, and PM_{10} from ships. Concentrations and percent with respect to the total amount of each species are reported. The maxima are derived by selecting cases with the largest ship impact (i.e. highest V concentration).

	$nssSO_4^{2-}$ ($(nssSO_4^{2-}/V)_{min}$=207)		**NO_3^-** ($(NO_3^-/V)_{min}$=12.5)		**OA** ($(OC/V)_{min}$=43.1)		**PM_{10}**	
	LMP	CGR	LMP	CGR	LMP	CGR	LMP	CGR
Average contribution μg/m^3 (%)	1.35 (34%)	2.1 (31%)	0.082 (4.5%)	0.13 (9.0%)	0.59 (15%)	0.78 (8.7%)	2.0 (11%)	3.0 (8.6%)
Maximum contribution μg/m^3 (%)	7.5 (69%)	8.8 (77%)	0.45 (62%)	0.53 (100%)	3.3 (99%)	3.3 (22%)	11.2 (50%)	12.7 (42%)

These percent contributions are higher than the annual average for the Mediterranean Region estimated by Viana et al. (2014). It has to be considered that these authors used data from harbour or coastal sites, which are highly affected by other sources in addition to ships, and where gas-to-particle conversion is still at its initial phase. Moreover, the percentages reported in this study are relative to the summer season, when the ship contribution in the Mediterranean region is highest (Becagli et al., 2012). The estimated lower limit for the ship contribution in cases with maximum ship impact was between 42% and 50% of the total PM_{10}.

Summary and conclusions

In this study we investigate the impact of the ship emissions to PM_{10} on measurements made at two sites in the central Mediterranean. The main objectives of the study were to unambiguously identify the tracers of ship emissions in the sampled aerosol, and to obtain a lower limit for the produced impact.

The PM_{10} samples were collected in summer 2013, as a contribution to the Chemistry and Aerosol Mediterranean Experiment, in parallel at Lampedusa and at Capo Granitola, respectively South and North of the main shipping route through the Mediterranean.

The identification of aerosol originating from ships was based on an integrated analysis combining chemical analyses, calculations of backward trajectories using a high

resolution regional model, and on tracking of ship traffic in the Mediterranean through the Automatic Identification System.
The main results of this study may be summarized as follows:

1. moderate and elevated values of V and Ni in the aerosol were unambiguously associated with the ship source; this attribution was based on:

   - the V to Ni ratio, which corresponds to what expected for heavy fuel oil combustion;

   - low amounts of La and Ce with respect to V, and La/Ce ratio similar to those in the UCC, which allowed to exclude power plants or refineries as sources significantly contributing to the observed aerosol;

   - coincidences between air mass trajectories and travelling ships;

2. in addition to travelling ships, also the planetary boundary layer vertical structure played an important role in determining the dispersion of aerosols from the ship source; temperature inversions appeared associated with elevated amounts of ship emissions tracers, suggesting that they favoured the build-up of aerosol concentration in the lowest atmospheric layers;

3. as expected, merchant ships (cargo and tankers) appeared to produce a larger impact on the measured aerosol than fishing vessels;

4. lower limits for the ratios $nssSO_4^{2-}/V$, NO_3^-/V, and OC/V, identifying the ship-dominated emission cases, were derived from the observations. The lower limits found at Lampedusa, which may be taken as a background site less affected by other types of anthropic emissions, are respectively 207, 12.5, and 44.1. These lower limits are expected to be season dependent;

5. by using these ratios, the lower limits to the contribution of the ship source to $nssSO_4^{2-}$, NO_3^-, OA, and to PM_{10} during the measurement campaign were estimated. Ship emissions contributed by at least 34% to the total amount of sulfate, by at least 5-9% to the total amount of NO_3^-, and by at least 9-15% to the total amount of organic aerosol. All these contributions correspond at least to 11% of PM_{10} at LMP (2.0 $\mu g/m^3$), and about 8.6% of PM_{10} at CGR (3.0 $\mu g/m^3$). In cases with largest ship impact, ships contributed up to about 12 $\mu g/m^3$ to PM_{10} in both sites, corresponding to 50% of PM_{10} at LMP and 42% at CGR;

6. Lampedusa is a small island in the southern sector of the central Mediterranean, relatively far from the main shipping Mediterranean route; thus, results at Lampedusa may be taken as representative of the impact of ships on the aerosol properties in a wide open sea area in the central Mediterranean during summer.

Acknowledgements

Measurements at Lampedusa were partly supported by the Italian Ministry for University and Research through the NextData and Ritmare projects.
We thank the Institute for Coastal Marine Environment of the National Research Council (IAMC-CNR), for hosting the instruments at Capo Granitola. Thanks are due to MarineTraffic (www.marinetraffic.com) for providing the information on the ship traffic in the Sicily Channel.

References

Agrawal, H., Malloy, Q.G.J., Welch, W.A., Miller, J.W., and Cocker, D.R.: In-use gaseous and particulate matter emissions from a modern ocean going container vessel, Atmos. Environ., 42, 5504−5510, 2008a.

Agrawal, H., Welch, W.A., Miller, J.W., and Cocker, D.R.: Emission measurements from a crude oil tanker at sea, Environ. Sci. Technol., 42, 7098−7103, 2008b.

Artuso, F., Chamard, P., Piacentino, S., Sferlazzo, D.M., De Silvestri, L., di Sarra, A., Meloni, D., and Monteleone, F.: nfluence of transport and trends in atmospheric CO_2 at Lampedusa, Atmos. Environ., 43, 3044-3051, 2009.

Ault, A. P., Gaston, C. J., Wang, Y., Dominguez, G., Thiemens, M. H., and Prather, K. A.: Characterization of the single particle mixing state of individual ship plume events measured at the port of los Angeles, Environ. Sci. Technol., 44, 1954–1961, 2010.

Becagli, S., Lazzara, L., Fani, F., Marchese, C., Traversi, R., Severi, M., di Sarra, A., Sferlazzo, D., Piacentino, S., Bommarito, C., Dayan, U., and Udisti, R.: Relationship between methanesulfonate (MS-) in atmospheric particulate and remotely sensed phytoplankton activity in oligo-mesotrophic Central Mediterranean Sea, Atmos. Environ., 79, 681-688, 2013.

Becagli, S., Sferlazzo, D. M., Pace, G., di Sarra, A., Bommarito, C., Calzolai, G., Ghedini, C., Lucarelli, F., Meloni, D., Monteleone, F., Severi, M., Traversi, R., and Udisti, R.: Evidence for heavy fuel oil combustion aerosols from chemical analyses at the island of Lampedusa: a possible large role of ships emissions in the Mediterranean, Atmos. Chem. Phys., 12, 3479–3492, doi:10.5194/acp-12-3479-2012, 2012.

Bove, M. C., Brotto, P., Calzolai, G., Cassola, F., Cavalli, F., Fermo, P., Hjorth, J., Massabò, D., Nava, S., Piazzalunga, A., Schembari, C., and Prati, P.: PM_{10} source apportionment applying PMF and chemical tracer analysis to ship-borne measurements in the Western Mediterranean, Atmos. Environ., 125, 140-151, doi:10.1016/j.atmosenv.2015.11.009, 2016.

Bove, M. C., Brotto, P., Cassola, F., Cuccia, E., Massabò, D., Mazzino, A., Piazzalunga, A., and Prati, P.: An integrated PM2.5 source apportionment study: Positive Matrix

828 Factorization vs. the Chemical Transport Model CAMx, Atmos. Environ., 94, 274–
829 286, doi:10.1016/j.atmosenv.2014.05.039, 2014.
830 Bozlaker, A., Buzcu-Güven, B., Fraser, M.P., and Chellam, S.: Insights into PM10 source
831 in Houston, Texas: Role of Petroleum refineries in enriching lanthanoid metal during
832 episodic emission events. Atmos. Environ., 69, 109-117, 2013.
833 doi:10.1016/j.atmosenv.2012.11.068.
834 Bowen, H. J. M.: Environmental chemistry of the elements, Academic Press, 1979.
835 Calzolai, G., Nava, S., Lucarelli, F., Chiari, M., Giannoni, M., Becagli, S., Traversi, R.,
836 Marconi, M., Frosini, D., Severi, M., Udisti, R., di Sarra, A., Pace, G., Meloni, D.,
837 Bommarito, C., Monteleone, F., Anello, F., and Sferlazzo, D.M.: Characterization of
838 PM10 sources in the central Mediterranean, Atmos. Chem. Phys., 15, 13939–13955,
839 2015.
840 Canepari, S., Farao, C., Marconi, E., Giovannelli, C., and Perrino, C.:. Qualitative and
841 quantitative determination of water in airborne particulate matter, Atmos. Chem.
842 Phys., 13, 1193–1202, doi:10.5194/acp-13-1193-2013, 2013.
843 Casasanta, G., di Sarra, A., Meloni, D., Monteleone, F., Pace, G., Piacentino, S., and
844 Sferlazzo, D.: Large aerosol effects on ozone photolysis in the Mediterranean.
845 Atmos. Environ., 45, 3937-3943, 2011.
846 Cassola, F., Ferrari, F., Mazzino, A., and Miglietta, M. M.: The role of the sea on the
847 flash floods events over Liguria (northwestern Italy), Geophys. Res. Lett., 43,
848 doi:10.1002/2016GL068265, 2016.
849 Cesari, D., Genga, A., Ielpo, P., Siciliano, M., Mascolo, G., Grasso, F.M., and Contini, D.:
850 Source apportionment of PM2.5 in the harbour–industrial area of Brindisi (Italy):
851 Identification and estimation of the contribution of in-port ship emissions, Sci. Total
852 Environ., 497–498, 392–400, 2014.
853 Chen, G., Huey, G., and Trainer, M.: An investigation of the chemistry of ship emission
854 plumes during ITCT 2002, J. Geophys. Res., 110, D10S90,
855 doi:10.1029/2004JD005236., 2005.
856 Coakley Jr., J. A. and Walsh, C. D.: Limits to the aerosol indirect radiative effect derived
857 from observations of ship tracks, J. Atmos. Sci., 59, 668–680, 2002.
858 Contini, D., Gambaro, A., Belosi, F., Pieri, S.D., Cairns, W.R.L., Donateo, A., Zanotto, E.,
859 and Citron, M.: The direct influence of ship traffic on atmospheric PM2.5, PM_{10} and
860 PAH in Venice, J. of Environ. Management, 92, 2119-2129, 2011.
861 Cooper, D.A.: Exhaust emissions from ships at berth, Atmos. Environ., 37, 3817−3830,
862 2003.
863 Corbett, J.J., Winebrake, J.J., Green, E.H., Kasibhatla, P., Eyring, V., and Lauer, A.:
864 Mortality from Ship Emissions: A Global Assessment, Environ. Sci., Technol., 41,
865 8512–8518, doi:10.1021/es071686z, 2007.
866 Dabdub, D., Air quality impacts of ship emission in south coast air basin of California.
867 Final report for State of California Air Resources Board Planning and Technical
868 support division, 2008.
869 Denjean, C., Cassola, F., Mazzino, A., Triquet, S., Chevaillier, S., Grand, N., Bourrianne,
870 T., Momboisse, G., Sellegri, K., Schwarzenbock, A., Freney, E., Mallet, M., and

871 Formenti, P.: Size distribution and optical properties of mineral dust aerosols
872 transported in the western Mediterranean, Atmos. Chem. Phys., 16, 1081-1104,
873 doi:10.5194/acp-16-1081-2016, 2016.
874 Derwent, R., Stevenson, D. S., Doherty, R. M, Collins, W. J., Sanderson, M. G., Amann,
875 M., and Dentener, F.: The contribution from ship emissions to air quality and acid
876 deposition in Europe, Ambio, 34, 54–59, 2005.
877 Devasthale, A., Krüger, O., and Graßl, H.: Impact of ship emissions on cloud properties
878 over coastal areas, Geophys. Res. Lett., 33, L02811, doi:10.1029/2005GL024470,
879 2006.
880 Diesch, J.M, Drewnick, F., Klimach, T., and Borrmann, S.: Investigation of gaseous and
881 particular emissions from various marine vessel types measured on the banks of the
882 Elbe in Northern Germany, Atmos. Chem. and Phys., 13, 3603–3618, 2013.
883 di Sarra, A., Di Biagio, C., Meloni, D., Monteleone, F., Pace, G., Pugnaghi, S., and
884 Sferlazzo, D.: Shortwave and longwave radiative effects of the intense Saharan dust
885 event of 25-26 March, 2010, at Lampedusa (Mediterranean sea), J. Geophys. Res.,
886 116, D23209, doi: 10.1029/2011JD016238, 2011.
887 di Sarra, A., Sferlazzo, D., Meloni, D., Anello, F., Bommarito, C., Corradini, S., De
888 Silvestri, L., Di Iorio, T., Monteleone, F., Pace, G., Piacentino, S., and Pugnaghi, S.:
889 Empirical correction of MFRSR aerosol optical depths for the aerosol forward
890 scattering and development of a long-term integrated MFRSR-Cimel dataset at
891 Lampedusa, Appl. Opt., 54, 2725-2737, 2015.
892 Donateo, A., Gregoris, E., Gambaro, A., Merico, A., Giua, R., Nocioni, A., and Contini,
893 D.: Contribution of harbour activities and ship traffic to PM2.5, particle number
894 concentrations and PAHs in a port city of the Mediterranean Sea (Italy), Environ. Sci.
895 Pollut. Res., 21, 9415–9429, doi:10.1007/s11356-014-2849-0, 2014.
896 Du, l., and Turner, J.: Using PM2.5 lanthanoid elements and nonparametric wind
897 regression to track petroleum refinery FCC emissions. Sci. Total. Environ., 529, 65-
898 71, doi:10.1016/j.scitotenv.2015.05.034, 2015.
899 Endresen, Ø., Sørgård, E., Sundet, J. K., Dalsøren, S. B., Isaksen, I. S. A., Berglen, T.
900 F., and Gravir, G.: Emissions from international sea transportation and
901 environmental impact, J. Geophys. Res., 108, 4560, doi:10.1029/2002JD002898,
902 2003.
903 Environmental Modeling Center: The GFS Atmospheric Model. NCEP Office Note 442.
904 National Oceanic and Atmospheric Administration, 2003.
905 Eyring, V., Koehler, H.W., van Aardenne, J., and Lauer, A.: Emissions from international
906 shipping: 1. The last 50 years, J. Geophys. Res., 110, D17305,
907 doi:10.1029/2004JD005619, 2005.
908 Gariazzo, C., Papaleo, V., Pelliccioni, A., Calori, G., Radice, P., and Tinarelli, G.:
909 Application of a Lagrangian particle model to assess the impact of harbour, industrial
910 and urban activities on air quality in the Taranto area, Italy, Atmos. Environ., 41,
911 6432-6444, 2007.

912 Grewal, D., and Haugstetter, H.: Capturing and sharing knowledge in supply chains in
913 the maritime transport sector: critical issues, Maritime Policy & Management, 169-
914 183, 2007.
915 Hellebust, S., Allanic, A., O'Connor, I.P., Jourdan, C., Healy, D., and Sodeau, J.R.:
916 Sources of ambient concentrations and chemical composition of PM2.5-0.1 in Cork
917 Harbour, Ireland, Atmos. Res., 95, 136-149. 2010.
918 Henderson, P. and Henderson, G. M.: The Cambridge Handbook of Earth Science Data,
919 Cambridge, University Press, Cambridge, 42–44, 2009.
920 Henne, S., Brunner, D., Folini, D., Solberg, S., Klausen, J., and Buchmann, B.:
921 Assessment of parameters describing representativeness of air quality in-situ
922 measurement sites, Atmos. Chem. Phys., 10, 3561–3581, 2010
923 Isakson, J., Persson, T.A., and Lindgren, E.S.: Identification and assessment of ship
924 emissions and their effects in the harbour of Goteborg, Sweden, Atmos. Environ. 35,
925 3659-3666. 2001.
926 Jiang, Q., Smith, R.B., and Doyle, J.: The nature of the mistral: Observation and
927 modelling of two MAP events, Q. J. R. Meteorol. Soc., 129, 857–875, 2003.
928 Jonsson, A.M, Westerlund, J., and Hallquist, M.: Size-resolved particle emission factors
929 for individual ships, Geophys. Res. Let., 38, L13809. DOI: 10.1029/2011GL047672,
930 2011.
931 Kouvarakis, G., Tsigaridis, K., Kanakidou, M., and Mihalopous, N.: Temporal variations
932 of surface regional background ozone over Crete Island in the southeast
933 Mediterranean, J. Geophys. Res., 105, 4399–4407, 2000.
934 Kulkarni, P., Chellam, S., and Fraser, M.P.: Lanthanum and lanthanides in atmospheric
935 fine particles and teir apportionment to refinery and petrochemical operations in
936 Houston, TX, Atmos. Environ., 40, 508-520, doi:10.1016/j.atmosenv.2005.09.063,
937 2006.
938 Lauer, A., Eyring, V., Hendricks, J., Jöckel, P., and Lohmann, U.: Global model
939 simulations of the impact of ocean-going ships on aerosols, clouds, and the radiation
940 budget, Atmos. Chem. Phys., 7, 5061–5079, doi:10.5194/acp-7-5061-2007, 2007.
941 Li, Z. and Aneja, V. P.: Regional analysis of cloud chemistry at high elevations in the
942 eastern United States, Atmos. Environ., 26A, 2001–2017, 1992.
943 Lloyd's Register Engineering Services, 1995. Marine Exhaust Emissions Research
944 Programme, London. pp. 63.
945 Lyyränen, J., Jokiniemi, J., Kauppinen, E.I., and Joutsensaari, J.: Aerosol
946 characterisation in medium-speed diesel engines operating with heavy fuel oils, J.
947 Aerosol Sci., 30, 771−784, 1999.
948 Mailler S., Menut, L., di Sarra, A. G., Becagli, S. Di Iorio, T., Bessagnet, B., Briant, R.,
949 Formenti, P.,Doussin, J.-F., Gómez-Amo, J. L., Mallet, M., Rea, G., Siour, G.,
950 Sferlazzo, D. M., Traversi, R., Udisti, R., and Turquety, S.: On the radiative impact of
951 aerosols on photolysis rates: comparison of simulations and observations in the
952 Lampedusa island during the ChArMEx/ADRIMED campaign, Atmos. Chem. Phys.,
953 16, 1219–1244, doi:10.5194/acp-16-1219-2016, 2016.

Mallet, M., Dulac, F., Formenti, P., Nabat, P., Sciare, J., Roberts, G., Pelon, J., Ancellet, G., Tanré, D., Parol, F., Denjean, C., Brogniez, G., di Sarra, A., Alados-Arboledas, L., Arndt, J., Auriol, F., Blarel, L., Bourrianne, T., Chazette, P., Chevaillier, S., Claeys, M., D'Anna, B., Derimian, Y., Desboeufs, K., Di Iorio, T., Doussin, J.-F., Durand, P., Féron, A., Freney, E., Gaimoz, C., Goloub, P., Gómez-Amo, J. L., Granados-Muñoz, M. J., Grand, N., Hamonou, E., Jankowiak, I., Jeannot, M., Léon, J.-F., Maillé, M., Mailler, S., Meloni, D., Menut, L., Momboisse, G., Nicolas, J., Podvin, T., Pont, V., Rea, G., Renard, J.-B., Roblou, L., Schepanski, K., Schwarzenboeck, A., Sellegri, K., Sicard, M., Solmon, F., Somot, S., Torres, B., Totems, J., Triquet, S., Verdier, N., Verwaerde, C., Waquet, F., Wenger, J., and Zapf, P.: Overview of the Chemistry-Aerosol Mediterranean Experiment/Aerosol Direct Radiative Forcing on the Mediterranean Climate (ChArMEx/ADRIMED) summer 2013 campaign, Atmos. Chem. Phys., 16, 455-504, doi:10.5194/acp-16-455-2016, 2016.

Marconi, M., Sferlazzo, D.M., Becagli, S., Bommarito, C., Calzolai, G., Chiari, M., di Sarra A., Ghedini, C., Gómez-Amo, J.L., Lucarelli F., Meloni D., Monteleone F., Nava S., Pace G., Piacentino S., Rugi F., Severi M., Traversi R., and Udisti R.: Saharan dust aerosol over the central Mediterranean Sea: PM_{10} chemical composition and concentration versus optical columnar measurements, Atmos. Chem. Phys., 14, 2039–2054, 2014.

Marmer, E. and Langmann, B.: Impact of ship emissions on Mediterranean summertime pollution and climate: A regional model study, Atmos. Environ., 39, 4659–4669, 2005.

Marmer, E., Dentener, F., Aardenne, J.V., Cavalli, F., Vignati, E., Velchev, K., Hjorth, J.,Moldanová, J., Fridell, E., Popovicheva, O., Demirdjian, B., Tishkova, V., Faccinetto, A., Focsa, C.: Characterisation of particulate matter and gaseous emissions from a large ship diesel engine, Atmos. Environ., 43, 2632−2641, 2009.

Mazzei F., D'Alessandro, A., Lucarelli, F., Nava, S., Prati, P., Valli, G., and Vecchi R.: Characterization of particulate matter sources in an urban environment, Sci. Tot. Environ., 401, 81–89, 2008.

Mentaschi, L., Besio, G., Cassola, F., and Mazzino, A.: Performance evaluation of WavewatchIII in the Mediterranean Sea, Ocean Model., 90, 82–94, doi:10.1016/j.ocemod.2015.04.003, 2015.

Micco, A., and Pérez, N.: Maritime transport costs and port efficiency. In: Bank, I.-A.D. (Ed.), Inter-american Development Bank, Santiago de Chile, p. 50. 2001.

Mihalopoulos, N., Stephanou, E., Kanakidou, M., Pilitsidis, S. and Bousquet, P.: Tropospheric aerosol ionic composition in the Eastern Mediterranean region, Tellus, 49B, 1 - 13, 1997.

Moldanová, J., Fridell, E., Popovicheva, O., Demirdjian, B., Tishkova, V., Faccinetto, A., and Focsa, C.: Characterisation of particulate matter and gaseous emissions from a large ship diesel engine, Atmos. Environ., 43, 2632−2641, 2009.

Moreno, T., Querol, X., Alastuey, A., Pey, J. Cruzminguillon, M., Perez, N., Bernabe, R., Blanco, S. Cardenas, B., and Gibbons, W.,: Lanthanoid geochemistry of urban atmospheric particulate matter, Environ. Sci. Technol., 42, 6502–6507, 2008a.

997 Moreno, T., Querol, X., Alastuey, A., and Gibbons, W.: Identification of FCC refinery
998 atmospheric pollution events using lanthanoid- and vanadium-bearing aerosols.
999 Atmos. Environ., 42, 7851-7861, doi:10.1016/j.atmosenv.2008.07.013, 2008b.
1000 Moreno, T., Querol, X., Castillo, S., Alastuey, A., Cuevas, E., Herrmann, L., Mounkaila,
1001 M., Elvira, J., and Gibbons, W.: Geochemical variation in aeolian mineral particles
1002 from the Sahara-Sahel dust corridor, Chemosphere, 65, 261-270,
1003 doi:10.1016/j.chemosphere.2006.02.052 2006..
1004 Murphy, S., Agrawal, H., Sorooshian, A., Padró, L.T., Gates, H., Hersey, S., Welch, W.
1005 A., Jung, H., Miller, J. W., Cocker, D.R. III, Nenes, A., Jonsson, H.H., Flagan, R.C.,
1006 and Seinfeld, J.H.: Comprehensive simultaneous shipboard and airborne
1007 characterization of exhaust from a modern container ship at sea, Environ. Sci.
1008 Technol., 43, 4626−4640, 2009.
1009 Olmez, I., and Gordon, G.E.: Rare earths: Atmospheric signatures for oil-fired power
1010 plants and refineries, Science, 6, 966–968, 1985.
1011 Pandolfi, M., Gonzalez-Castanedo, Y., Alastuey, A., Rosa, J.d.l., Mantilla, E., Campa,
1012 A.S.d.l., Querol, X., Pey, J., Amato, F., and Moreno, T.: Source apportionment of
1013 PM_{10} and PM2.5 at multiple sites in the strait of Gibraltar by PMF: impact of shipping
1014 emissions, Environ. Sci. Pollution Res., 18, 260-269, 2011.
1015 Schembari, C., Bove, M. C., Cuccia, E., Cavalli, F., Hjorth, J., Massabò, D., Nava, S.,
1016 Udisti, R., and Prati, P.: Source apportionment of PM10 in the Western
1017 Mediterranean based on observations from a cruise ship, Atmos. Environ., 98, 510-
1018 518, 2014.
1019 Sellitto, P., Zanetel, C., di Sarra, A., Salerno, G., Tapparo, A., Meloni, D., Pace, G.,
1020 Caltabiano, T., Briole, P., and Legras, B.: The impact of Mount Etna sulfur emissions
1021 on the atmospheric composition and aerosol properties in the central Mediterranean:
1022 a statistical analysis over the period 2000-2013 based on observations and
1023 Lagrangian modelling, Atmos. Environ., 148, 77-88, 2017.
1024 Shah, S.D., Cocker, D.R., Miller, J.W., and Norbeck, J.M.: Emission rates of particulate
1025 matter and elemental and organic carbon from in-use diesel engines, Environ. Sci.
1026 Technol., 38, 2544–2550, 2004.
1027 Simo, R., Colom-Altes, M., Grimalt, J. O. and Albaiges, J.: Background levels of
1028 atmospheric hydrocarbons, sulphate and nitrate over the Western Mediterranean.
1029 Atmos. Environ., 29, 1487-1500, 1991.
1030 Sippula, O., Hokkinen, J., Puustinen, H., Yli-Piril¨a, P., and Jokiniemi J: Comparison of
1031 particle emissions from small heavy fuel oil and wood-fired boilers, Atmos. Environ.,
1032 43, 4855–4864, 2009.
1033 Sippula, O., Stengel, B., Sklorz, M., Streibel, T., Rabe, R., Orasche, J., Lintelmann, J.,
1034 Michalke, B., Abbaszade, G., Radischat, C., Gröger, T., Schnelle-Kreis, J., Harndorf,
1035 H., and Zimmermann R.: Particle emissions from a marine engine: chemical
1036 composition and aromatic emission profiles under various operating conditions,
1037 Environ. Sci. Technol., 48, 11721−11729, 2014.
1038 Skamarock, W. C., Klemp, J. B., Dudhia, J., Gill, D. O., Barker, D. M., Huang, X. Z.,
1039 Wang, W., and Powers, J. G.: A Description of the Advanced Research WRF Version

3. Technical report. Mesoscale and Microscale Meteorology Division, NCAR, Boulder, Colorado, 2008.
Solomos, S., Amiridis, V., Zanis, P., Gerasopoulos, E., Sofiou, F. I., Herekakis, T., Brioude, J., Stohl, A., Kahn, R. A., and Kontoes, C.: Smoke dispersion modeling over complex terrain using high resolution meteorological data and satellite observations – The FireHub platform, Atmos. Environ., 119, 348-361, 2015.
Stein, A. F., Draxler, R. R, Rolph, G. D., Stunder, B. J. B., Cohen, M. D., and Ngan, F.: NOAA's HYSPLIT atmospheric transport and dispersion modeling system, Bull. Amer. Meteor. Soc., 96, 2059-2077, doi:10.1175/BAMS-D-14-00110.1, 2015.
Stern, N.,:The Economics of Climate Change: The Stern Review. Cambridge and New York, Cambridge University press. 2007.
Trozzi, C., Vaccaro, R., and Nicolo, L.: Air pollutants emissions estimate from maritime traffic in the Italian harbours of Venice and Piombino, Sci. Total Environ., 169, 257–263, 1995.
Tsyro, S. G.: To what extent can aerosol water explain the discrepancy between model calculated and gravimetric PM_{10} and $PM_{2.5}$?, Atmos. Chem. Phys., 5, 515–532, 2005.
Turpin, B.J. and Lim H.J.: Species contributions to PM2.5 mass concentrations: Revisting common assumptions for estimating organic mass, Aerosol Sci. Technol., 35, 602–610, 2001.
Viana, M., Amato, F., Alastuey, A., Querol, X., Moreno, T., Santos, S.G.D., Herce, M.D., and Fernández-Patier, R.: Chemical tracers of particulate emissions from commercial shipping, Environ. Sci. Tech., 43, 7472-7477, 2009.
Viana, M., Hammingh, P., Colette, A., Querol, X., Degraeuwe, B., de Vlieger, I., van Aardenne, J.: Impact of maritime transport emissions on coastal air quality in Europe, Atmos. Environ., 90 96-105, 2014.
Viana, M., Kuhlbusch, T.A.J., Querol, X., Alastuey, A., Harrison, R.M., Hopke, P.K., Winiwarter, W., Vallius, M., Szidat, S., Prévôt, A.S.H., Hueglin, C., Bloemen, H., Wåhlin, P., Vecchi, R., Miranda, A.I., Kasper-Giebl, A., Maenhaut, W., and Hitzenberger, R.: Source apportionment of particulate matter in Europe: a review of methods and results, J. Aerosol Sci., 39, 827-849, 2008.
World Health Organization (WHO): Health Effects of Particulate Matter, Policy Implications for Countries in Eastern Europe, Caucasus and Central Asia, Regional office for Europe, Copenhagen, Denmark, 2013.
Wu, C., Huang, X. H. H., Ng, W. M., Griffith, S. M., and Yu, J. Z.: Inter-comparison of NIOSH and IMPROVE protocols for OC and EC determination: Implications for inter-protocol data conversion, Atmos. Meas. Tech. Discuss., doi:10.5194/amt-2016-116, in review, 2016